Gas-phase ion chemistry and ab initio theoretical study of phosphine. II. Reactions of PH + with PH 3

Paola Antoniotti, Lorenza Operti, Roberto Rabezzana, Glauco Tonachini, and Gian Angelo Vaglio

Citation: The Journal of Chemical Physics **109**, 10853 (1998); doi: 10.1063/1.477782
View online: http://dx.doi.org/10.1063/1.477782
View Table of Contents: http://scitation.aip.org/content/aip/journal/jcp/109/24?ver=pdfcov
Published by the AIP Publishing

Gas-phase ion chemistry and *ab initio* theoretical study of phosphine. II. Reactions of PH^+ with PH_3

Paola Antoniotti, Lorenza Operti,[a] Roberto Rabezzana, Glauco Tonachini,[b] and Gian Angelo Vaglio
Dipartimento di Chimica Generale ed Organica Applicata, Università degli Studi di Torino, Corso Massimo d'Azeglio 48, 10125 Torino, Italy

(Received 19 May 1998; accepted 16 September 1998)

The gas-phase ion chemistry of phosphine has been investigated by *ab initio* theoretical calculations and experimental techniques. Following a previous study of H and H_2 loss pathways from the $^3P–PH_3^+$ adduct (generated by $^3P^+$ reacting with PH_3), the quantum chemical study of these processes has been extended to the ion–molecule reactions starting from $^2PH^+$ reacting with PH_3, as observed by ion trapping. In these experiments, PH^+ reacts to give $P_2H_n^+$ $(n=2,3)$ product ions, with loss of H_2 or H in different pathways, and also reacts in charge–exchange processes to form PH and PH_3^+. Moreover, elimination of two hydrogen molecules has been observed leading to the formation of the P_2^+ ion species. All these processes take place at similar rates, their constants ranging from 1.2 to 5.5×10^{-10} cm^3 $molecule^{-1}$ s^{-1}. The geometrical structures and energies of transition structures, reaction intermediates, and final products have been determined by *ab initio* theoretical methods. The initial step is formation of the $^2HP–PH_3^+$ adduct. Then, a hydrogen atom can be directly lost either from dicoordinated or tetracoordinated phosphorus, to give $^3P–PH_3^+$ or $^1HP{=}PH_2^+$, respectively. Alternatively, one hydrogen can first undergo a displacement from the latter to the former P atom to give $^2H_2P–PH_2^+$. This migration can then be followed by P–H bond dissociation, yielding again $^1HP{=}PH_2^+$. Dissociation of H_2 can also occur, from either the initial $HPPH_3^+$ or rearranged $H_2P–PH_2^+$ isomeric ions, yielding the $^2HP{=}PH^+$ or $^2H_2P{=}P^+$ ions, respectively. These last species are related by a H-migration process. A last H_2 loss from $H_2P{=}P^+$ produces $^2P_2^+$. Other pathways were explored, but proved not to be viable. The heats of formation of the $P_2H_n^+$ $(n=0–4)$ ionic species have also been computed and reported with the experimental data in the literature. © *1998 American Institute of Physics.* [S0021-9606(98)30548-6]

I. INTRODUCTION

The combined application of advanced experimental methods and *ab initio* quantum chemical calculations have permitted a strong development in gas-phase ion chemistry.[1–5] Product distributions, reaction mechanisms, and rate constants of ion–molecule reactions have been determined as well as ion structures, reaction profiles, and thermochemical data.[6–19]

These studies have improved the understanding of processes of interest mainly in research fields concerning the atmospheric chemistry,[9] the formation processes and reactivity of interstellar media,[20] and the preparation of solid materials by activation of volatile systems.[6–8] Considering this last point, ion–molecule clustering reactions are suited for investigating the chain propagation and the consequent formation of amorphous solids by deposition from gaseous mixtures.

In previous papers the mechanisms related to the first steps of x-ray assisted chemical vapor deposition (CVD) from gaseous systems have been investigated by mass spectrometric methods.[21] In particular, the germane–phosphine[7] and silane–phosphine[8] systems have been studied to investigate the formation of ionic species containing new Ge–P and Si–P bonds. With the aim to evaluate the conditions under which preparation of germanium or silicon doped with phosphorus could be performed from appropriate volatile mixtures containing PH_3, we have recently reported the results of *ab initio* quantum chemical calculations on the reaction pathways of P^+ with PH_3,[5] as observed by ion trap mass spectrometry, and in this paper we report the theoretical and experimental results on the reaction pathways of PH^+ with PH_3.

A significant contribution to fundamental chemistry is also given by the calculation of heats of formation of ions containing two phosphorus atoms.

II. EXPERIMENT

Phosphine was commercially supplied by Union Carbide Industrial Gases N.V. (Belgium) at electronic grade degree of purity. Prior to use, it was introduced into a flask, containing anhydrous sodium sulfate as drier agent, which was connected to the gas inlet system of the instrument. Helium was obtained commercially in extra-high purity and was used without further purification. The manifold and the lines were baked out frequently in order to reduce the water background in the trap.

[a]Electronic mail: OPERTI@CH.UNITO.IT
[b]Electronic mail: glauco@2500.ch.unito.it

A Finnigan ITMS ion trap mass spectrometer was used for all experiments, which were run at 333 K. The theory, instrumentation and methodology of ion trap mass spectrometry have been discussed elsewhere.[5–8] The pressures were read by a Bayard–Alpert ionization gauge and were typically $2-5\times10^{-7}$ Torr for phosphine and about 5×10^{-4} Torr for helium. The real pressure in the trap was calculated considering the relative sensitivity of the ion gauge with respect to different gases[22] and a calibration factor.[8] The scan modes for ion–molecule reaction experiments, in which reaction mechanisms and rate constants are determined, have been previously described in detail together with the calculation procedures.[5–8] In kinetic experiments, isolation of the precursor ions was generally obtained by a superimposition of radio frequency (rf) and direct current (dc) voltages. In same cases, experiments were also performed in which ions were selectively stored by resonance ejection, without any dc voltage which could add energy to the ions under examination. The similarity of the rate constants determined by these two isolation methods indicates that collisional cooling is effective in removing most of the internal energy as is also evidenced by the single exponential behavior observed in calculating the reaction rate constants. In all experiments ionization was obtained by bombardment with an electron beam at ionization time in the range 1–10 ms. Afterwards, reactions take place during a time suitable to maximize the abundances of ions to be collected. Isolation of the selected ion species, their reactions with neutral molecules present in the trap for convenient reaction times, and acquisition are the successive steps.

III. THEORETICAL METHODS

The study of the H atom rearrangement and H or H_2 loss processes in the $P_2H_4^+$ doublet species was carried out by determining, on the relevant energy hypersurface, the critical points corresponding to stable and transition structures. This was accomplished through unconstrained gradient optimization[23] of the geometrical parameters at the complete active space (CAS) multiconfiguration self-consistent field (MCSCF)[24] and UMP2[25(a)] (second-order unrestricted Møller–Plesset perturbation theory) levels of theory. UMP2 energies were refined by spin projection by using the method of Chen and Schlegel [PUMP2 (projected UMP2) values].[25(b)] In this computation the polarized split-valence shell 6-31G(d)[26] basis set was used. The UMP2/6-31G(d) geometries were characterized as energy minima or first order saddle points (transition structures) by diagonalization of the analytically computed Hessian (vibrational frequencies calculations).[27] In the Figures the interatomic distances are reported in Ångströms and angles in degrees. The UMP2/6-31G(d) geometries were used to recompute the relative energies by quadratic configuration interaction calculations at the QCISD(T) level,[28] in conjunction with the more extended basis set 6-311G($3df$,$2p$).[26] The basis set superposition error (BSSE)[29] was estimated at both UMP2/6-31G(d) and QCISD(T)/6-311G($3df$,$2p$) levels, in relation with the first process, in which the HP–PH_3^+ adduct is formed from HP^+ and PH_3, and also for the charge–exchange process, yielding HP and PH_3^+. Zero-point vibrational energies[27,29] (ZPE) were computed at the UMP2/6-31G(d) level. The GAUSSIAN94 suite of programs[30] was used throughout.

IV. RESULTS AND DISCUSSION

A. Mass spectrometric determinations

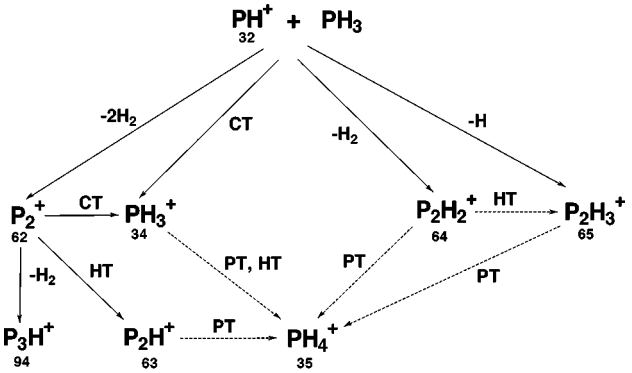

Scheme 1

Scheme 1 reports the mechanisms of ion–molecule reactions starting from the primary ion of phosphine, PH^+. The dashed arrows indicate pathways common to reactions of the primary ion P^+, which have been already published.[5,31] In the first reaction step, four products are observed, PH_3^+, P_2^+, $P_2H_2^+$, and $P_2H_3^+$, which are formed following different pathways. These represent the charge transfer (CT) process and condensation of a phosphine molecule followed by elimination of two hydrogen molecules ($-2H_2$), or of a hydrogen molecule ($-H_2$), or of a hydrogen atom ($-H$). In turn, the secondary ions can react further with neutral PH_3 showing among others hydrogen transfer (HT) and proton transfer (PT) processes. The Scheme was built in successive experiments in which every primary ion was selectively stored for variable reaction times up to 500 ms, and the ion species formed during these delay times were detected. Then, the identified product ions were isolated and reacted, detecting the new products. The number of reaction steps which can be determined was limited by the loss of instrumental sensitivity at long reaction times and by the low intensity of ions to be isolated.

The thermochemical data available in the literature[5,32,33] indicate that the following path

$$PH^+ + PH_3 \rightarrow P_2H_2^+ + H_2, \tag{1}$$

in which a hydrogen molecule is lost, is the most exothermic process observed for reactions of PH^+ with phosphine, the enthalpy of reaction being negative by 39, 32, or 31 kcal mol^{-1}, using $\Delta H°_f(P_2H_2^+)=253$,[5] 260,[5] or 261 kcal mol^{-1},[33] respectively. Indeed, condensation reaction with elimination of H_2 is a very common path in gaseous ion chemistry, as it has been evidenced in ion–molecule clustering of silane[34] and germane.[6] The charge–exchange reaction is also thermodynamically favored, as it is exothermic by ~7 kcal mol^{-1}; while the condensation process which takes place with loss of a hydrogen atom is almost thermoneutral ($\Delta H_r^0=1$, 6, or -6 kcal mol^{-1}), the heat of formation of

TABLE I. Rate constants for reactions of PH^+ and its product ions in self-condensation of PH_3.[a]

Reaction	k_{exp}	Σk_{exp}	k_{ADO}[b]	Efficiency[c]
$PH^+ + PH_3 \rightarrow PH_3^+ + PH$	5.5			
$PH^+ + PH_3 \rightarrow P_2^+ + 2H_2$	2.1			
$PH^+ + PH_3 \rightarrow P_2H_2^+ + H_2$	4.1			
$PH^+ + PH_3 \rightarrow P_2H_3^+ + H$	1.2	12.9	11.46	1.12
$PH_3^+ + PH_3 \rightarrow PH_4^+ + PH_2$[d]	*12.4*	*12.4*	*11.28*	*1.10*
$P_2^+ + PH_3 \rightarrow PH_3^+ + P_2$	11.6			
$P_2^+ + PH_3 \rightarrow P_2H^+ + PH_2$	0.4	12.0	9.93	1.21
$P_2H_2^+ + PH_3 \rightarrow PH_4^+ + P_2H$[d]	*8.0*			
$P_2H_2^+ + PH_3 \rightarrow P_2H_3^+ + PH_2$[d]	*0.8*	*8.8*	*9.87*	*0.89*
$P_2H_3^+ + PH_3 \rightarrow PH_4^+ + P_2H_2$	5.4	5.4	9.85	0.55

[a]Rate constants are expressed as 10^{-10} cm^3 molecule^{-1} s^{-1}; experiments were run at 333 K; uncertainty is within 20%.
[b]Rate constants have been calculated according to the ADO theory.
[c]Efficiency has been calculated as the ratio k_{exp}/k_{ADO}.
[d]Rate constants already published in Ref. 5 and reported here for sake of completeness.

$P_2H_3^+$ ranging from 234[33] to 246 kcal mol^{-1}.[5] The reaction pathway occurring with elimination of two hydrogen molecules is quite unusual and it has not been observed previously in similar systems. Moreover, on the basis of thermochemical data it seems endothermic by about 17 kcal mol^{-1}. It is more difficult to draw analogous considerations on the secondary processes as the enthalpies of formation of two-phosphorus containing neutral species or three-phosphorus ions are not available in the literature. Therefore, it is possible to calculate the heat of reaction only for the hydrogen transfer processes ($P_2^+ \rightarrow P_2H^+$, $P_2H_2^+ \rightarrow P_2H_3^+$), which, surprisingly, are endothermic by 12–28 kcal mol^{-1} and by 6–21 kcal mol^{-1}, respectively, taking the enthalpies of formation of the two-phosphorus ions from Ref. 5 or 33.

In Table I the rate constants for reactions of PH^+ and its product ions with phosphine are shown. The same Table reports the collisional rate constants calculated according to the ADO (average dipole orientation) theory[35] and the efficiencies of reaction, which are the ratio between the experimental and calculated rate constants. Reactions written in italic refer to data already published in the preceeding paper on P^+.[5] Both primary and secondary reactions display very high efficiencies (in some cases even higher than unity, probably due to experimental errors) which indicate that generally the ion species under examination react at collisional rates. The condensation process of PH^+ with phosphine, in which a hydrogen molecule is lost, occurs with a higher rate constant (4.1×10^{-10} cm^3 molecule^{-1} s^{-1}) with respect to reaction in which two hydrogen molecules (2.1×10^{-10} cm^3 molecule^{-1} s^{-1}) or a hydrogen atom (1.2×10^{-10} cm^3 molecule^{-1} s^{-1}) are eliminated. Among secondary reactions, the fastest processes lead to the formation of PH_4^+, which is unreactive under the experimental conditions here used. Condensation of P_2^+ to give P_3H^+ takes place so slowly that its rate constant is too small to be determined with a good reliability.

B. Theoretical study of the reactions

Several chemical processes, which can in principle take place, were examined. In the following list they are numbered as in Scheme 2 (italic numerals associated to the arrows). The ensuing subsections will also follow this order. In Scheme 2 intermediate species and transition structures are labeled by bold numerals.

(1) The first process is the initial formation, from HP^+ and PH_3, of the doublet $HP–PH_3^+$ adduct (left of Scheme 2).

(2) Then the charge–exchange process is considered, which produces the HP and PH_3^+ species (top-left of Scheme 2).

(3) Two different hydrogen atom dissociations from $^2HP–PH_3^+$ giving either $^3P–PH_3^+$ (3*a*, bottom-left) or $HP{=}PH_2^+$ (3*b*, center), singlet or triplet; one hydrogen molecule dissociation from $^2HP–PH_3^+$, giving $^2HP{=}PH^+$ (3*c*, top) in its cis and trans isomeric forms.

(4) H migration in the initial adduct, from the tetracoordinated phosphorus atom to the other one, giving $^2H_2P–PH_2^+$ (bottom). This species appears in two geometries, with P atoms in a pyramidal or planar arrangement. The last one is much less stable and is not displayed in Scheme 2.

(5) The ensuing hydrogen atom dissociation from this last species, yielding again $HP{=}PH_2^+$ (5*a*, center), already produced via path 3*b*, or hydrogen molecule dissociation, giving $^2P{=}PH_2^+$ (5*b*, right).

(6) From $HP{=}PH_2^+$ (center), H loss can produce either $HP{=}PH^+$ (6*a*, top), already encountered via pathway 3*c*, or $P{=}PH_2^+$ (6*b*, right), which has just been reported as the product of process 5*b*.

(7) The ion $P{\equiv}PH^+$ could be obtained by three different fragmentations: from $HP{=}PH_2^+$ by hydrogen molecule dissociation (7*a*, center to top-right); from $P{=}PH_2^+$ (right), by H atom dissociation (7*b*); from $HP{=}PH^+$, by H loss (top, 7*c*). All these processes are indicated by dashed arrows (see below), as well as that leading to P_2^+, through H loss from $P{\equiv}PH^+$.

(8) $P{=}PH_2^+$ (right) is related to trans $HP{=}PH^+$ (top) by a H migration process (8*a*). H_2 dissociation from $P{=}PH_2^+$ would give P_2^+ (8*b*).

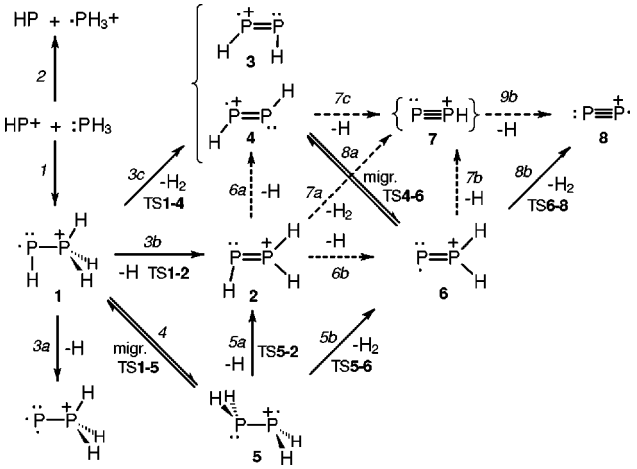

Scheme 2

The first part of the study had the purpose of ascertaining

TABLE II. Total and relative energies (hartree and kcal mol^{-1}) for the reaction $PH^+ + PH_3$.

	Structure	CASSCF/6-31G(d)	ΔE
1	$^2HP_2H_3^+$	−683.536 116	0.0
	$^3P_2H_3^+$	−682.932 438	66.17[a]
TS1-2	$(H)H_2P_2H^+$(H dissociation TS)	−683.436 829	62.30
2	$^1HP_2H_2^+$	−682.939 590	61.68[a]
	$^3HP_2H_2^+$ ''W''	−682.895 125	89.58[a]
3	cis-$^2H_2PH^+$	−682.298 846	57.06[b]
4	trans-$^2HP_2H^+$	−682.153 866	148.04[b]
TS1-4	$HP_2H(H_2)^+$ (H_2 dissociation TS)	−683.428 213	67.71[b]
TS1-5	$HP(H)PH_2^+$ (H migration TS)	−683.450 320	53.84
5	$^2H_2P_2H_2^+$	−683.517 847	11.46
TS5-6	$H_2P_2(H_2)^+$ (H_2 dissociation TS)	−683.417 828	74.23
6	$^2P_2H_2^+$	−682.327 538	39.06[b]
TS6-8	$P_2(H_2)^+$ (H_2 dissociation TS)	−683.234 744	97.28[b]
TS4-6	$HP(H)P^+$ (H migration TS)	−682.281 643	67.85[b]
8	$^2P_2^+$	−681.128 462	72.15[c]

[a]$E(H) = -0.498\,233$ added in.
[b]$E(H_2) = -1.146\,338$ added in.
[c]$E(H_2)$ added twice.

the nature of the wave function in the different processes, in order to assess to what extent a single reference wave function had to be expected to provide a qualitatively acceptable description of the potential-energy hypersurface. The critical point geometries were thus determined at the CAS-MCSCF/6-31G(d) level of theory, using an active space defined by nine electrons in nine orbitals.[36] Total and relative energies are reported in Table II. No structure resulted to be endowed with diradical character (two configurations with comparable weights). Instead, for all critical points of interest, the MCSCF wave function is characterized by the dominance of one configuration, with coefficient 0.95–0.97 in most cases (cis-HP_2H and P_2H_2 have the lowest coefficients: 0.92 and 0.93, respectively).

Thus, a single configuration seems to provide, for all structures of interest, a rather adequate reference in perturbative calculations. Therefore, in a second phase, the critical point geometries were re-determined by UMP2 optimizations, in conjunction with the same basis sets used in the previous calculations. Finally, the energetics were better assessed by QCISD(T) calculations. In the following, the reaction pathways introduced above will be discussed.

1. Formation of doublet $HP-PH_3^+$

The initial step is the reaction of a doublet HP^+ ion with phosphine, which brings about the formation of a doublet $HP-PH_3^+$ adduct of C_s symmetry, whose structure, **1**, is shown in Fig. 1.

The P–P bond length, ~2.2 Å, is close to that found for neutral P_2H_4[37] and has essentially the nature of a single PP bond. The CAS-MCSCF wave function for this species has one dominant configuration, corresponding to single occupancy of one p-π orbital which is orthogonal to the symmetry plane and essentially localized on that phosphorus atom which carries one hydrogen. The MCSCF and UMP2 optimizations produced quite similar geometries (bond lengths differ by 0.01 Å, angles by 1° at most). The UMP2 computations are based on preceding unrestricted Hartree–Fock

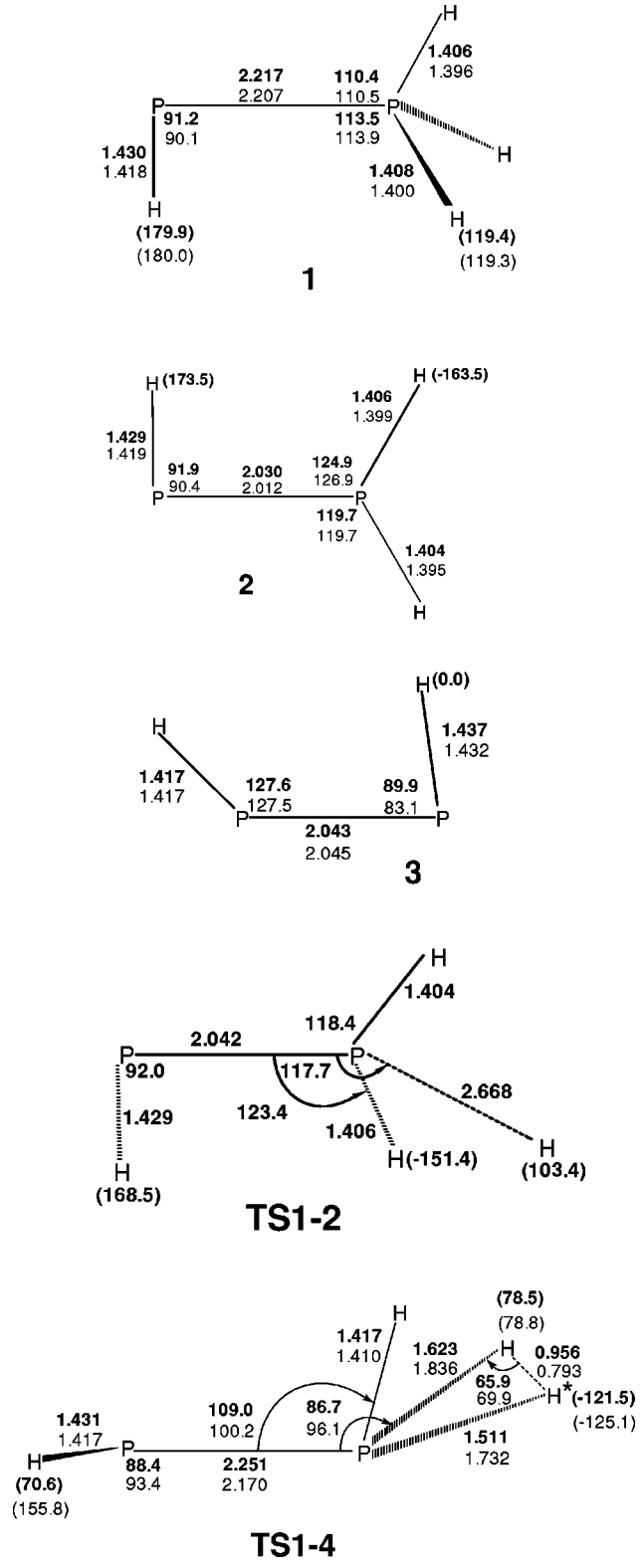

FIG. 1. (**1**) Initial $HPPH_3^+$ adduct of C_S simmetry; (**TS1-2**) H dissociation TS from **1**, leading to **2**; (**2**) $HPPH_2^+$ intermediate; (**TS1-4**) H_2 dissociation TS from **1**, leading to **4**, trans-$HPPH^+$; (**3**) cis-$HPPH^+$ intermediate. Bond distances are in ångström, and bond angles in degrees. Dihedral angles (in parentheses) are defined as HPP**H**, where the reference **H** determines with the two P atoms the sheet plane or HHP**H** in the case of the starred hydrogen in **TS1-4**. CAS-MCSCF/6-31G(d) (bold) and MP2/6-31G(d) (plain) values are shown.

(UHF) calculations, which might be significantly contaminated by spin multiplicities higher than the doublet. Therefore, Table III reports also spin-projected second-order Moller–Plesset (MP2)[37] energy values. However, in this case, the total spin eigenvalue $\langle S^2 \rangle$ appears to be rather close to 0.75 (Table III), and consequently contamination is not large.

It is important to assess the extent of the energy gain acquired by the system in proceeding from the two separate reactants to the adduct **1**, because all the processes that can follow in principle are surely feasible if the relevant energy barriers are lower than the quantity of kinetic energy attained by the system in this first stage. In this respect, the PUMP2/6-31G(d) estimate, -86.2 kcal mol^{-1}, and the QCISD(T)/6-31G($3df$,$2p$) one, -87.0 kcal mol^{-1} (Tables III and IV), can be expected to be affected to some extent by a basis set superposition error. Its magnitude is estimated to be 5.0 kcal mol^{-1}, at the PUMP2 level, and 2.3 kcal mol^{-1}, at the QCISD(T) level. For ideal collisions tending to zero kinetic energy, this estimate provides a limiting energy value of 81.2 kcal mol^{-1} (for the PUMP2 barriers), or 84.7 kcal mol^{-1} (for the QCI estimate of the same barriers).

2. Charge exchange process

The following equation:

$$HP^+ + PH_3 \rightarrow HP + PH_3^+, \tag{2}$$

describing an electron-transfer process, corresponds to an energy difference of -15.7 kcal mol^{-1} at the PUMP2 level of theory (Table III), and -8 kcal mol^{-1}, at the QCISD(T) level of theory (Table IV).

3. H *and* H_2 *dissociations from* $HP-PH_3^+$

The initial adduct can undergo hydrogen atom loss in two different ways. If H dissociates from the P atom bearing a single H (pathway $3a$), then $^3P-PH_3^+$ is obtained, whose chemical evolution was already dealt with in the previous paper on P^+ (where its geometry is displayed as structure $1a$).[5] This fragmentation is estimated to require overcoming a barrier of 66.2 kcal mol^{-1}, at the PUMP2 level, or 78.5 kcal mol^{-1}, at the QCISD(T) level, which is just the energy associated to this step, because the reverse process has no barrier.

On the other hand, H can be lost by the PH_3 group. The relevant transition structure is shown in Fig. 1 as structure **TS1-2**. It has been determined at the MCSCF level, because no transition structure is found again, at the UMP2 level. In this case (pathway $3b$), a new ion is formed, $^1HP{=}PH_2^+$, whose additional fragmentations will be discussed below (see paragraph 6). Its planar structure, **2**, is also shown in Fig. 1. The PP bond length, ~2.0 Å, is shorter than that found for **1** and can be considered as typical of a PP double bond. The ion **2** is located 58.4 kcal mol^{-1} above **1**, at the PUMP2 level, or 64.5 kcal mol^{-1}, at the QCISD(T) level. This species could be obtained in principle either as a singlet, or a triplet. The latter was dealt with in the first paper,[5] where a structure with the PH and PH_2 groups pointing in opposite directions (''*Y*'' conformation, in which the hybrid P lobes are anti) resulted to be an easily attainable intermediate (structure $1c$). This *Y* triplet, however, is found in the present case to be high in energy, 84.9 kcal mol^{-1} above **1**, at the PUMP2 level, and 94.9 kcal mol^{-1}, at the QCISD(T) level, i.e., 5–10 kcal mol^{-1} above the thresholds just defined. $^3HP-PH_2$ can also be found in a ''*W*'' conformation, i.e., with the PH and PH_2 groups pointing from the same side (here the hybrid P lobes are syn). Its energy is even higher (Table IV).

H_2 dissociation (pathway $3c$) yields the $^2HP{=}PH^+$ ion, in its cis and trans forms. To obtain it, the H_2 dissociation process requires 61.6 kcal mol^{-1}, at the PUMP2 level, or 52.6 kcal mol^{-1}, at the QCISD(T) level. In correspondence of this barrier transition structure **TS1-4** is found (Fig. 1). Of the two isomeric structures, the cis, **3**, is also shown in Fig. 1. The trans, **4**, was already discussed in the previous paper,[5] where its geometry is displayed as $2e$. It is noteworthy that the total spin eigenvalue $\langle S^2 \rangle$ is now larger than 0.79 for all these structures (Table III), showing that a larger spin contamination, with respect to **1**, is present in the wave function relevant to geometry optimizations. In both isomers the P–P bond length is ~2.0 Å, which is essentially typical of a PP double bond. These energy minima have very different stability, the trans isomer being the more stable. Trans $^2HP{=}PH^+$ is located 43.2 kcal mol^{-1} above **1**, at the PUMP2 level, or 46.6 kcal mol^{-1}, at the QCISD(T) level. Cis $^2HP{=}PH^+$ is higher in energy, 58.3 kcal mol^{-1} above **1**, at the PUMP2 level, or 56.0 kcal mol^{-1}, at the QCISD(T) level. This is also the case in which the dominance of a single configuration in the CAS-MCSCF wave function is less sharp, its coefficient being 0.924.

In summary, all these processes require overcoming energy barriers which result to be lower than the limiting values assessed above. Therefore, all these reaction channels can be considered open to the system.

4. H *atom migration connecting* $HP-PH_3^+$ *and* $H_2P-PH_2^+$

The initial adduct can also transform to the isomeric ion $H_2P-PH_2^+$ by a H-migration from one P to the other (pathway 4). The rearrangement transition structure **TS1-5** is displayed in Fig. 2. Also this process, requiring 52.1 kcal mol^{-1} at the PUMP2 level, or 44.9 kcal mol^{-1}, at the QCISD(T) level, appears to be feasible. In this doublet case, the $\langle S^2 \rangle$ value is larger than 0.80 (Table III), and consequently contamination is larger than in the preceding cases.

Actually, $H_2PPH_2^+$ exists in two geometries. Of the two isomeric $H_2PPH_2^+$ ions, one is planar. As it resulted to be a high-energy structure (99.4 kcal mol^{-1}) at the PUMP2 level, it was not investigated any further. The other one, shown in Fig. 2 as structure **5**, is just 4.7 kcal mol^{-1} (PUMP2) above **1**, and 5.9 kcal mol^{-1}, at the QCISD(T) level. This modest endoergicity defines the barrier height for the backward process: 47.1 kcal mol^{-1}, at the PUMP2 level, and 39.0 kcal mol^{-1}, at the QCISD(T) level. The P–P bond length is slightly shorter than 2.2 Å, while for **1** it was slightly larger. It seems, however, to be still closer in nature to a single than to a double bond. Also for this minimum $\langle S^2 \rangle$ is close to

TABLE III. Total and relative energies (hartree and kcal mol^{-1}) for the reaction $PH^+ + PH_3$.

		$\langle S^2\rangle$[e]	UMP2	ΔE	PUMP2	ΔE	ZPE[f]	ΔZPE
	$PH^+ + PH_3$		−683.543 987	86.1	−683.545 597	86.2	19.3	−4.1
			−683.551 782[g]	81.2[g]	−683.553 644[g]	81.2[g]		
	$PH_3^+ + PH$		−683.567 792	71.1	−683.570 529	70.5	19.2	−4.2
			−683.573 975[g]	67.2[g]	−683.576 773[g]	66.6[g]		
1	$^2HP_2H_3^+$	0.7636	−683.681 151	0.0	−683.682 935	0.0	23.4	0.0
	$^3P_2H_3^+$	2.0215	−683.077 346	66.2[a]	−683.079 245	66.2[a]	18.2	−5.3
2	$^1HP_2H_2^+$	0.0	−683.091 712	57.2[a]	−683.091 712	58.4[a]	17.4	−6.0
	$^3HP_2H_2^+$ ''*Y*''	2.0315	−683.046 773	85.4[a]	−683.049 363	84.9[a]	15.5	−6.9
	$^3HP_2H_2^+$ ''*W*''	2.0245	−683.040 260	89.5[a]	−683.042 521	89.2[a]	15.5	−7.9
3	cis-$^2HP_2H^+$	0.7942	−682.443 858	58.5[b]	−682.445 948	58.3[b]	9.7	−13.7
4	trans-$^2HP_2H^+$	0.7939	−682.465 814	44.7[b]	−682.469 986	43.2[b]	13.6	−9.8
TS1-4	$HP_2H(H_2)^+$ (H_2 dissociation TS)	0.7921	−683.581 612	62.5	−683.584 716	61.6	20.3	−3.2
TS1-5	$HP(H)PH_2^+$ (H migration TS)	0.8010	−683.596 318	−53.2	−683.599 903	52.1	22.6	−0.8
5	$^2H_2P_2H_2^+$	0.7977	−683.671 370	6.1	−683.675 463	4.7	23.1	−0.3
TS5-6	$H_2P_2(H_2)^+$ (H_2 dissociation TS)	0.7673	−683.580 023	63.5	−683.582 123	63.3	19.6	−3.8
6	$^2P_2H_2^+$	0.7996	−682.473 732	39.7[b]	−682.476 517	39.1[b]	17.8	−5.6
TS6-8	$P_2(H_2)^+$ (H_2 dissociation TS)	1.0316	−682.389 925	92.3[b]	−682.399 298	87.5[b]	8.7	−14.7
TS4-6	$HP(H)P^+$ (H migration TS)	0.9668	−682.427 016	69.0[b]	−682.433 906	65.8[b]	9.3	−14.1
8	$^2P_2^+$	0.7551	−681.284 430	68.0[c]	−682.285 172	68.7[c]	0.9	−22.5
	$^1PPH^+$	0.0	−681.895 156	90.1[d]	−681.895 156	91.2[d]	4.6	−18.8
	$^3PPH^+$	2.0154	−681.829 379	131.4[d]	−681.831 118	131.4[d]	5.2	−18.2

[a]$E(H) = -0.498\,233$ added in.
[b]$E(H_2) = -1.144\,141$ added in.
[c]$E(H_2)$ added twice.
[d]$E(H)$ and $E(H_2)$ added in.
[e]Eigenvalues of spin operator at the UHF/6-31G(d) level of theory.
[f]Zero-point energies (kcal mol^{-1}) at the MP2/6-31G(d) level of theory.
[g]With counterpoise correction of the basis set superposition error.

TABLE IV. Total and relative energies (hartrees and kcal mol^{-1}) for the reactions of PH^+ with PH_3.

	Structure	QCISD(T)/6-311G($3df$,$2p$)[a]	ΔE
	$^2PH^+ + PH_3$	−683.733 095	87.0
		−683.736 775[b]	84.7[b]
	$^3PH + {}^2PH_3^+$	−683.745 775	79.0
		−683.749 108[b]	77.0[b]
1	$^2HP_2H_3^+$	−683.871 755	0.0
	$^3P_2H_3^+$	−683.246 821	78.5[c]
2	$^1HP_2H_2^+$	−683.269 096	64.5[c]
	$^3HP_2H_2^+$ (''*Y*'', anti P lobes)	−683.220 760	94.9[c]
	$^3HP_2H_2^+$ (''*W*'', syn P lobes)	−683.214 660	98.7[c]
3	cis-$^2HP_2H^+$	−682.611 745	56.0[d] 163.4[e]
4	trans-$^2HP_2H^+$	−682.626 628	46.6[d] 154.1[e]
TS1-4	$HP_2H(H_2)^+$ (H_2 dissociation TS)	−683.787 996	52.6
TS1-5	$HP(H)PH_2^+$ (H migration TS)	−683.800 249	44.9
5	$^2H_2P_2H_2^+$	−683.862 291	5.9
TS5-6	$H_2P_2(H_2)^+$ (H_2 dissociation TS)	−683.786 465	53.5
6	$^2P_2H_2^+$	−682.636 717	40.3[d] 147.7[e]
TS6-8	$P_2(H_2)^+$ (H_2 dissociation TS)	−682.572 634	80.5[d]
TS4-6	$HP(H)P^+$ (H migration TS)	−682.602 439	61.8[d]
8	$^2P_2^+$	−681.410 383	75.1[f]
	$^1PPH^+$	−682.032 235	106.0[g]
	$^3PPH^+$	−681.975 918	141.3[g]

[a]Calculated using UMP2/6-31G(d) optimized geometries.
[b]With counterpoise correction of the basis set superposition error.
[c]$E(H) = -0.499\,810$ added in.
[d]$E(H_2) = -1.170\,809$ added in.
[e]$E(H)$ added in twice.
[f]$E(H_2)$ added in twice.
[g]$E(H)$ and $E(H_2)$ added in.

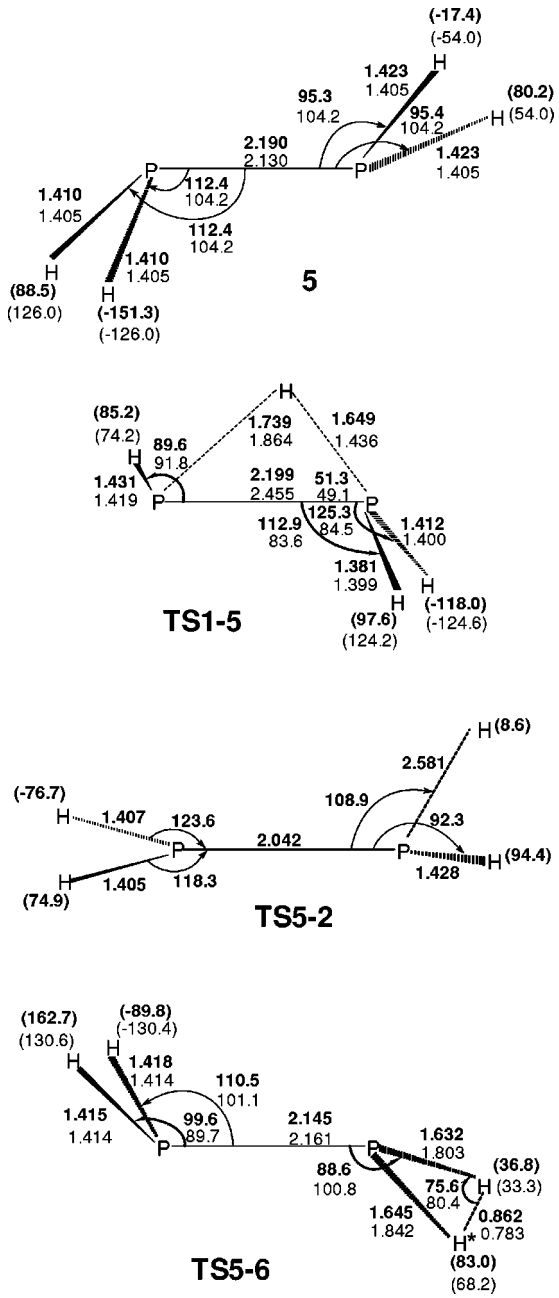

FIG. 2. (**TS1-5**) H migration TS connecting **1** to the $H_2PPH_2^+$ intermediate **5** by a [1,2] shift; (**5**) $H_2PPH_2^+$ rearranged ion; (**TS5-2**) H dissociation TS from **5**, leading to **2**; (**TS5-6**) H_2 dissociation TS from **5**, leading to **6**. Bond distances are in ångström, and bond angles in degrees. Dihedral angles (in parentheses) are defined as HPP**X**, where the reference **X** (dummy atom) is bound to one P atom and perpendicular to the PP bond, lying on the sheet plane. In **TS5-6** the dihedral angle of the starred hydrogen is defined as HHP**X**. CAS-MCSCF/6-31G(*d*) (bold) and MP2/6-31G(*d*) (plain) values are shown.

0.80 (Table III). Further reactions, originating from **5**, will be described in the following subsection.

5. H *and* H_2 *dissociations from* $H_2PPH_2^+$

From the $H_2PPH_2^+$ ion, H and H_2 dissociation can take place (pathways $5a$ and $5b$, respectively). H loss leads to the ion $HP{=}PH_2^+$, already seen as the result of pathway $3b$, and has no related UMP2 transition structure. However, one transition structure is found at the MCSCF level: its geometry, **TS5-2**, is shown in Fig. 2. In contrast, H_2 dissociation presents at both theory levels one transition structure, displayed in Fig. 2 as structure **TS5-6**. It leads to the ion $P{=}PH_2^+$, **6** in Scheme 2, which was already encountered in the first paper (structure $2d$).[5] A barrier of 58.6 kcal mol^{-1} is found at the PUMP2 level, that becomes 47.6 kcal mol^{-1} at the QCISD(T) level. The ion $P{=}PH_2^+$ could in principle result also from H dissociation in $HP{=}PH_2^+$, as will be discussed presently.

6. H *dissociation from* $HP{=}PH_2^+$

This ion (Fig. 1, structure **2**), obtained through pathways $3b$ or $5a$, can undergo three different fragmentations, either losing a H atom or a H_2 molecule (Scheme 2, center). If one H were lost from the P atom bearing two hydrogens, pathway $6a$, the $HP{=}PH^+$ ion could be obtained (in the two isomeric forms **3** and **4** already discussed). If, on the other hand, H departs from the P atom bearing a single hydrogen, then pathway $6b$ is followed. By this step the ion $P{=}PH_2^+$, just encountered as the product **6** of pathway $5b$, could be obtained again. No transition structures were detected for these H-loss processes. So, the related energetics are just dictated by the energy differences between **2** and **4**, or **2** and **6** (Tables III and IV). It is not surprising that obtaining **3**, **4**, or **6** by two subsequent H losses (pathways $3b$ or $5a$ as first step) is prohibitively expensive in energy terms. In fact, Table IV shows that these ions can be reached only through H_2 losses (compare the leftmost and rightmost ΔE values for these entries). For this reason both second H losses relevant to the formation of these ions (pathways $6a$ and $6b$) are marked as dashed arrows in Scheme 2.

7. H *and* H_2 *dissociations yielding* $^+$PPH

H_2 dissociation in $HP{=}PH_2^+$ (pathway $7a$, dashed arrow) would lead to $^1HPP^+$. This linear ion (Scheme 2, **7**) has the following bond lengths: $PP = 1.918_5$ Å, $PH = 1.415$ Å (UMP2). The PP bond length suggests that this ion has basically a PP triple bond. All pathways converging onto **7**, although possible in principle, are indicated in Scheme 2 by dashed arrows. This is because $^1HPP^+$ lies high enough in energy to justify not to search for related transition structures, which would be located well beyond the defined threshold. $^1PPH^+$ is in fact located 91.2 kcal mol^{-1} above **1** (PUMP2) or 106.0 kcal mol^{-1} [QCISD(T)]. The bent ion $^3PPH^+$ (dealt with the previous paper as structure $3c$[5]) lies even higher. Their energies are reported in Tables III and IV for sake of completeness. So, also loss of one H atom from $P{=}PH_2^+$ could produce $P{\equiv}PH^+$, as indicated in Scheme 2 (pathway $7b$, dashed arrow). The $HP{=}PH^+$ ion as well (top) is related to $P{\equiv}PH^+$ by a H loss process (pathway $7c$, dashed arrow).

8. H_2 *dissociation and* H *atom migration in* $^+P{=}PH_2$

The ion $P{=}PH_2^+$ (Scheme 2, **6**) is related to trans-$(HP{=}PH)^+$ (Scheme 2, **4**) by a H migration process (pathway $8a$). The relevant transition structure **TS4-6** is shown in Fig. 3. Its energy is 26.7 kcal mol^{-1} above **4** at the PUMP2

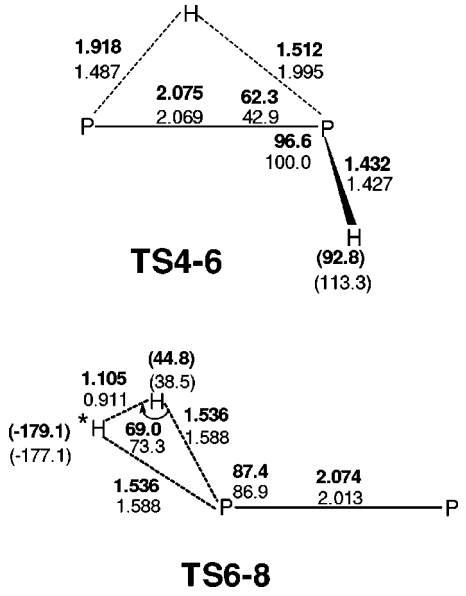

FIG. 3. (**TS4-6**) H migration TS connecting trans-$HPPH^+$ (**4**) to PPH_2^+ (**6**) by a [1,2] shift; (**TS6-8**) H_2 dissociation TS from **6**, leading to **8**. Bond distances are in ångström, and bond angles in degrees. In **TS4-6**, the dihedral angle (in parentheses) is defined as HPP**H**, where the reference **H** determines with the two P atoms the sheet plane. In **TS6-8** are defined as HPP**X**, where the reference **X** (dummy atom) is bound to one P atom and perpendicular to the PP bond, lying on the sheet plane and HHP**X** for the starred hydrogen. CAS-MCSCF/6-31G(d) (bold) and MP2/6-31G(d) (plain) values are shown.

level. This transition structure, in which $\langle S^2 \rangle$ is ~0.97, corresponds to one of the more contaminated doublet encountered in this study. The barrier becomes 21.5 kcal mol^{-1} at the QCISD(T) level. The $P{=}PH_2^+$ ion **6** can undergo a hydrogen molecule loss (pathway 8b) via transition structure **TS6-8** (Fig. 3). This process gives $^2P_2^+$ (**8** in Scheme 2). PP bond length in **8** is 1.979 Å at the MCSCF level and 1.933 Å at the UMP2 level (triple PP bond). H_2 dissociation is endoergic, with respect to **6**, by 29.6 kcal mol^{-1} at the PUMP2 level, or 34.8 at the QCISD(T) level. The energy barrier for this step is 48.4 (PUMP2), while a value of 40.2 is obtained by single-point QCISD(T) computation on the UMP2 TS geometry. Inspection of Table IV shows that these values bring pathway 8b close to the energy threshold defined in Sec. I.

It can be commented, at the end of this section, that all H_2 dissociation transition structures encountered (**TS1-4**, **TS5-6**, **TS6-8**) exhibit a symmetry lowering with respect to the reference ions. The reason can be traced back, by analysis of the MCSCF wave function, to the presence of a real crossing between two electronic states of different symmetry, that can be observed only if symmetry is enforced along a ''pseudo-reaction pathway''. Therefore, the reaction is allowed to take place in correspondence of an avoided crossing only if the symmetry lowering permits the two states to mix. No further details will be given here, because this feature was already discussed in the first paper.[5]

In Fig. 4 an overall picture is reported of the features described (H detachment processes are shown on the right and H_2 dissociations on the left).

9. Thermochemistry

For all structures of ions studied, included those not directly accessible in the present reaction system [$^3HP_2H_2^+$(''Y''), $^3HP_2H_2^+$(''W''), $^1PPH^+$, $^3PPH^+$], formation enthalpies (ΔH_f°) were calculated by four different methods. The results are reported in Table V.

Method A relies on tabulated experimental formation enthalpies.[32] These are combined with the computed standard reaction enthalpy relevant to the formation of a particular ion $P_2H_n^+$, and provide an estimate of its ΔH_f°. In the previous paper[5] the differences between ΔH_f° values obtained by using either scaled[38] or unscaled MP2/6-31G(d) frequencies appeared to be insignificant, the largest change being 0.3 kcal mol^{-1}. Therefore, it was chosen to report in the first column of Table V $\Delta H_f^\circ(P_2H_n^+)$ values for which the MP2/6-31G(d) vibrational frequencies, used to compute the thermal correction, were scaled as suggested in Ref. 38. These values have no decimal figures, because $\Delta H_f^\circ(P^+)$, used in method *A*, is reported in Ref. 32 without any.

The second estimate (Method *B*) more heavily relies on computed data. It was obtained by the method proposed by Pople *et al.*,[39] with two modifications already adopted in the first paper: (i) The QCISD(T)/6-311G(3df,2p) energies (reported in Table IV) were directly used throughout, instead of those obtained as in Eq. (1) of Ref. 39; (ii) instead of the ZPE correction to the energy, the full thermal correction was applied (as outlined in Ref. 38).[5] Again, scaled frequencies were used. In this column the entries corresponding to the ions discussed in the previous paper on P^+ can also be found.[5] They have been recomputed in order to allow a comparison with those of the present study on a homogeneous ground, given that the basis set used there, in the QCISD(T) computations, was less extended [6-311G(2d,2p)].

The third and fourth methods are more recent and belong to the same category. They are the popular G2[40] and complete basis set (CBS)[41] composite techniques, which rely on the combination of different *ab initio* calculations, and which have been found to perform very satisfactorily in estimating heats of formation and related thermochemical quantities. Their relative performances have been recently compared over a set of 166 closed shell radical or charged small noncyclic molecules.[42] The CBS method has been employed in the present study in the CBS-Q formulation.

The enthalpies of formation of the $P_2H_n^+$ ions previously obtained by experimental methods[32,33] are also reported for comparative purposes. In considering these data, it must be remembered that Fehlner and Callen determined the ΔH_f° values from the appearance potentials of ions generated from P_2H_4.[33] Therefore, heats of formation result to be typically overestimated, due to a significant kinetic shift.[43]

When available, alternative estimates are also offered,[32] which, in turn, are not well established values, as commented by the authors of the volume themselves. The computations have, of course, limitations, but the experimental values suffer from some uncertainty too: both are contributions to a better assessment of the ΔH_f° values. Moreover, it must be noted the overall consistency of the computed values, whichever the method.

Finally, the enthalpy of the charge–exchange reaction,

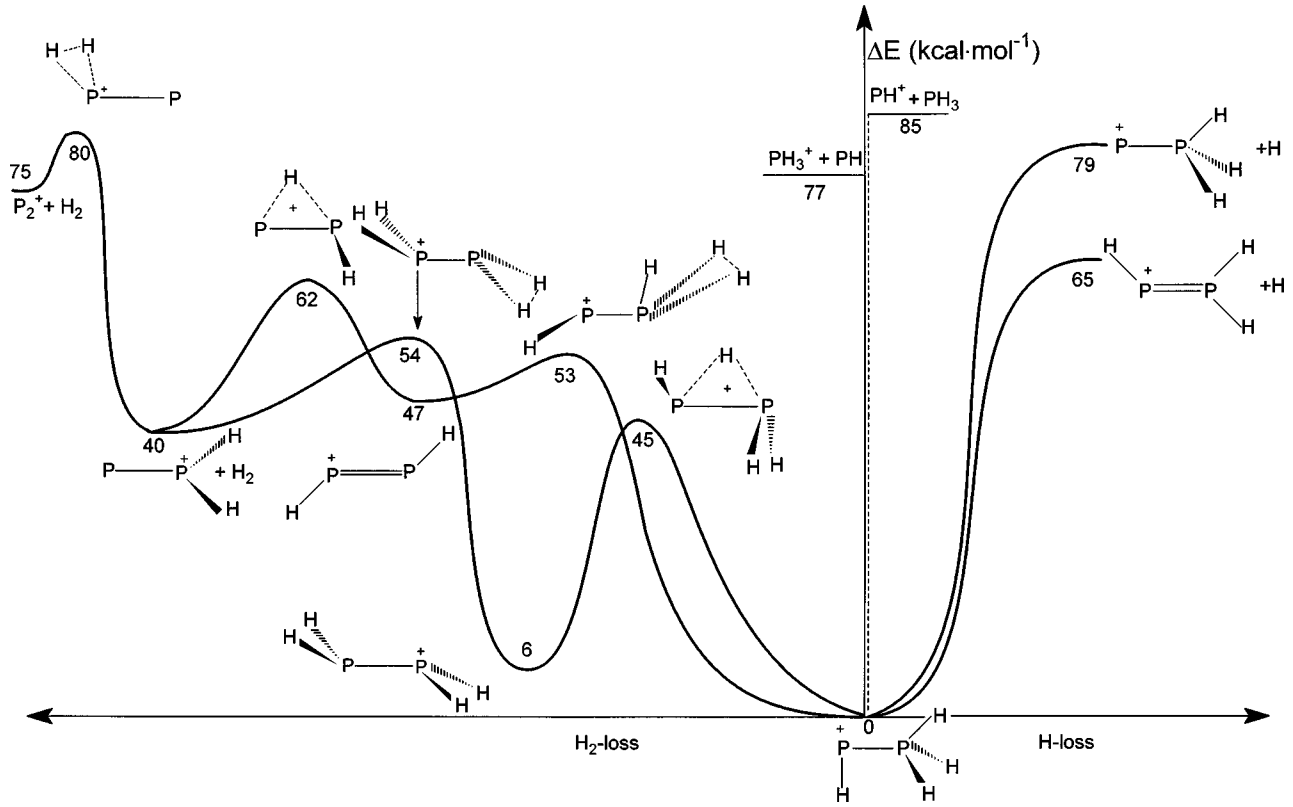

FIG. 4. QCISD(T) energy profiles (energy values are reported as integers; reference can be made to Table IV). Right: H atom dissociation pathways. Left: H atom migration pathway from **1** to **5** and H_2 molecule dissociation pathways. Only viable pathways are reported.

-8.1 kcal mol^{-1}, computed using the QCISD(T) energies and the MP2 thermal corrections, is quite close to that calculated on the basis of the formation enthalpies recently reported in the literature (-7 kcal mol^{-1}).[32]

V. CONCLUSIONS

Hydrogen atom and hydrogen molecule dissociations from the initial adduct HP–PH_3^+, produced by collision of doublet HP^+ onto phosphine, as well as from other intermediates obtained from it, have been investigated by correlated *ab initio* methods. The best energy estimates are collected in Table IV. The potential energy released in the adduct formation is estimated to be $\sim$85 kcal mol^{-1}. This value sets a reference value for determining which rearrangement and cleavage products are attainable, in the limit of zero kinetic energy.

The overall picture emerging from this study is summarized in Scheme 2. Viable pathways are indicated by arrows.

TABLE V. Heats of formation[a] of the $P_2H_n^+$ ions (kcal mol^{-1}).

		$\Delta H°_f$				
	Structure	*A*	*B*	*G*2	CBS-Q	Experimental[b]
1	$^2HP_2H_3^+$	203	211	208	211	216, 219[c]
5	$^2H_2P_2H_2^+$	214	217	214	216	
2	$^1HP_2H_2^+$	216	219	216	218	234
	$^3P_2H_3^+$	230	235.5	234	235	
	$^3HP_2H_2^+$ (''*Y*'')	246	251	249	249	
	$^3HP_2H_2^+$ (''*W*'')	249	254	252	254	
6	$^2P_2H_2^+$	245	248	245	246	261
4	trans-$^2HP_2H^+$	253.5	257	253	252	
3	cis-$^2HP_2H^+$	259	262	260	260	
	$^1PPH^+$	254	257	255	255	289
	$^3PPH^+$	289	292	292	291	
8	$^2P_2^+$	276	280	279	278	309, 277.2[c]

[a]Calculated using QCISD(T)/6-311G(3*df*,2*p*)//UMP2/6-31G(*d*) energies; thermal correction computed using scaled UMP2/6-31G(*d*) frequencies, as suggested in Ref. 36.
[b]Fehlner and Callen, Ref. 33.
[c]Lias *et al.*, Ref. 32.

Dashed arrows mark those processes which have been considered, but result to require an energy which goes beyond the mentioned threshold. Thus, an initial rearrangement of $HP{-}PH_3^+$ (**1**) to $H_2P{-}PH_2^+$ (**5**) appears to be quite viable. Then, from both these isomeric ions, H_2 dissociations can take place (diagonal arrows). These produce new ions: $HP{=}PH^+$ (**4**) from the former isomer, and $P{=}PH_2^+$, (**6**) from the latter. Also these ions are related by a H-migration process. In contrast with the H_2 dissociations, pathways leading to the same ions **4** and **6** through two succeeding H losses require too much energy. However, both processes lead in the first step to the intermediate ion $HP{=}PH_2^+$ (**2**), which results indeed to be attainable. A last H_2 loss from $P{=}PH_2^+$ (**6**) yields $P{\equiv}P^+$ (**8**). This comes out to be the only viable pathway to P_2^+. In fact, alternative processes leading in principle to $P{\equiv}PH^+$ (**7**), by H loss from $HP{=}PH^+$ (**4**) or $P{=}PH_2^+$ (**6**) are too energy-requiring. The same is true for H_2 dissociation from the ion $HP{=}PH_2^+$ (**2**). Therefore, $P{\equiv}PH^+$ (**7**) does not appear to be reachable.

Analogously and even in a more pronounced way with respect to the results obtained for reactions of P^+ with PH_3, processes starting from $PH^+ + PH_3$ occur at similar rate constants, their largest ratio being 4.6. This behavior is in agreement with the small energy differences of the four main pathways determined by theoretical calculations.

Finally, the enthalpies of formation of the $P_2H_n^+$ ions were calculated theoretically. The obtained estimates, although subject to known limitations, can be deemed a useful contribution, in view of the uncertainties often present in the experimentally determined values.

ACKNOWLEDGMENTS

The authors thank MURST and University of Torino for financial support.

[1] N. G. Adams and L. M. Babcock, in *Advances in Gas Phase Ion Chemistry* (Jai, Greenwich, 1996), Vol. 2.
[2] F. Cacace, Pure Appl. Chem. **69**, 227 (1997).
[3] D. Schröder, C. Heinemann, W. Koch, and H. Schwarz, Pure Appl. Chem. **69**, 273 (1997).
[4] P. B. Armentrout and T. Baer, J. Phys. Chem. **100**, 12866 (1996).
[5] P. Antoniotti, L. Operti, R. Rabezzana, M. Splendore, G. Tonachini, and G. A. Vaglio, J. Chem. Phys. **107**, 1491 (1997).
[6] P. Benzi, L. Operti, G. A. Vaglio, P. Volpe, M. Speranza, and R. Gabrielli, J. Organomet. Chem. **354**, 39 (1988); **373**, 289 (1989); Int. J. Mass Spectrom. Ion Processes **100**, 647 (1990); L. Operti, M. Splendore, G. A. Vaglio, P. Volpe, M. Speranza, and G. Occhiucci, J. Organomet. Chem. **433**, 35 (1992); L. Operti, M. Splendore, G. A. Vaglio, and P. Volpe, Spectrochim. Acta A **49**, 1213 (1993); Organometallics **12**, 4509 (1993); **12**, 4516 (1993); L. Operti, M. Splendore, G. A. Vaglio, A. M. Franklin, and J. F. J. Todd, Int. J. Mass Spectrom. Ion Processes **136**, 25 (1994); J. F. Gal, R. Grover, P. C. Maria, L. Operti, R. Rabezzana, G. A. Vaglio, and P. Volpe, J. Phys. Chem. **98**, 11978 (1994); L. Operti, R. Rabezzana, G. A. Vaglio, and P. Volpe, J. Organomet. Chem. **509**, 151 (1996).
[7] P. Benzi, L. Operti, R. Rabezzana, M. Splendore, and P. Volpe, Int. J. Mass Spectrom. Ion Processes **152**, 61 (1996).
[8] P. Antoniotti, L. Operti, R. Rabezzana, G. A. Vaglio, P. Volpe, J. F. Gal, R. Grover, and P. C. Maria, J. Phys. Chem. **100**, 155 (1996).
[9] F. Cacace and M. Speranza, Science **265**, 208 (1994).
[10] F. Cacace, F. Pepi, and F. Grandinetti, J. Phys. Chem. **98**, 8009 (1994).
[11] M. T. Bowers, A. G. Marshall, and F. W. McLafferty, J. Phys. Chem. **100**, 12897 (1996).
[12] I. Haller, J. Phys. Chem. **94**, 4135 (1990).
[13] M. L. Mandich, W. D. Reents, Jr., and M. F. Jarrold, J. Chem. Phys. **88**, 1703 (1988); M. L. Mandich, W. D. Reents, Jr., and K. D. Kolenbrander, *ibid.* **92**, 437 (1990); M. L. Mandich, M. L. and W. D. Reents, Jr., *ibid.* **95**, 7360 (1991); W. D. Reents, Jr. and M. L. Mandich, *ibid.* **96**, 4429 (1992).
[14] K. Raghavachari, J. Chem. Phys. **88**, 1688 (1988); **92**, 452 (1990); **95**, 7373 (1991); **96**, 4440 (1992).
[15] K. A. Nguyen, M. S. Gordon, and K. Raghavachari, J. Phys. Chem. **98**, 6704 (1994).
[16] J. Berkowitz, L. A. Curtiss, S. T. Gibson, J. P. Greene, G. L. Hillhouse, and J. A. Pople, J. Chem. Phys. **84**, 375 (1986).
[17] J. M. H. Pakarinen, P. Vainiotalo, C. L. Stumpf, D. T. Leeck, P. K. Chou, and H. I. Kenttämaa, J. Am. Soc. Mass Spectrom. **7**, 482 (1996).
[18] E. M. Cruz, X. Lopez, M. Ayerbe, and J. M. Ugalde, J. Phys. Chem. **101**, 2166 (1997).
[19] E. M. Cruz, X. Lopez, M. Sarobe, F. P. Cossío, and J. M. Ugalde, J. Comput. Chem. **18**, 9 (1997).
[20] S. Petrie, H. Becker, V. Baranov, and D. K. Bohme, Astrophys. J. **476**, 191 (1997); S. Petrie and D. K. Bohme, *ibid.* **436**, 411 (1994); Mon. Not. R. Astron. Soc. **268**, 103 (1994).
[21] M. Speranza, Trends Organomet. Chem. **1**, 35 (1994).
[22] M. Decouzon, J. F. Gal, P. C. Maria, and A. S. Tchinianga, Personal communication.
[23] H. B. Schlegel, in *Computational Theoretical Organic Chemistry*, edited by I. G. Csizsmadia and R. Daudel (Reidel, Dordrecht, The Netherlands, 1981), p. 129; H. B. Schlegel, J. Chem. Phys. **77**, 3676 (1982); H. B. Schlegel, J. S. Binkley, and J. A. Pople, *ibid.* **80**, 1976 (1984); H. B. Schlegel, J. Comput. Chem. **3**, 214 (1982).
[24] M. A. Robb and R. H. A. Eade, ''Single and Multi-configuration SCF methods,'' in Procedings of the NATO-ASI on Computational Theoretical Organic Chemistry, edited by R. Daudel (Reidel, Dordrecht, Holland, 1980).
[25] (a) C. Møller and M. S. Plesset, Phys. Rev. **46**, 618 (1934); J. S. Binkley and J. A. Pople, Int. J. Quantum Chem. **9**, 229 (1975); The computations were carried out without the frozen core approximation; (b) W. Chen and H. B. Schlegel, J. Chem. Phys. **101**, 5957 (1994), and references therein.
[26] R. Ditchfield, W. J. Hehre, and J. A. Pople, J. Chem. Phys. **56**, 2252 (1972); P. C. Hariharan and J. A. Pople, Theor. Chim. Acta **28**, 213 (1973); M. M. Francl, W. J. Pietro, W. J. Here, J. S. Binkley, M. S. Gordon, D. J. Defrees, and J. A. Pople, J. Chem. Phys. **77**, 3654 (1982); K. Raghavachari, J. S. Binkley, R. Seeger, and J. A. Pople, *ibid.* **72**, 650 (1980); A. D. Mc Lean and G. S. Chandler, *ibid.* **72**, 5639 (1980).
[27] J. A. Pople, A. P. Scott, M. W. Wong, and L. Radom, Isr. J. Chem. **33**, 345 (1993).
[28] J. A. Pople, M. Head-Gordon, and K. Raghavachari, J. Chem. Phys. **87**, 5968 (1987).
[29] See for instance: W. J. Hehre, L. Radom, P. v. R. Schleyer, and J. A. Pople, in *Ab Initio Molecular Orbital Theory* (Wiley, New York, 1985); S. M. Bachrach and A. Streitwieser Jr., J. Am. Chem. Soc. **106**, 2283 (1984); see also the discussion in: J. H. van Lenthe, C. C. M. van Duijneveldt-van de Rijdt and F. B. van Duijneveldt, in *Ab Initio Methods in Quantum Chemistry II*, edited by K. P. Lawley (Wiley, New York, 1987), p. 521, and references therein.
[30] GAUSSIAN, M. J. Frisch, G. W. Trucks, H. B. Schlegel, P. M. W. Gill, B. G. Johnson, M. A. Robb, J. R. Cheeseman, T. Keith, G. A. Petersson, J. A. Montgomery, K. Raghavachari, M. A. AlLaham, V. G. Zakrzewski, J. V. Ortiz, J. B. Foresman, J. Cioslowski, B. B. Stefanov, A. Nanayakkara, M. Challacombe, C. Y. Peng, P. Y. Ayala, W. Chen, M. W. Wong, J. L. Andres, E. S. Replogle, R. Gomperts, R. L. Martin, D. J. Fox, J. S. Binkley, D. J. Defrees, J. Baker, J. P. Stewart, M. Head-Gordon, C. Gonzalez, and J. A. Pople, Gaussian Inc., Pittsburgh, PA, 1995.
[31] D. Holtz, J. L. Beauchamp, and J. R. Eyler, J. Am. Chem. Soc. **92**, 7045 (1970).
[32] S. G. Lias, J. E. Bartmess, J. F. Liebman, J. L. Holmes, R. D. Levin, and W. G. Mallard, J. Phys. Chem. Ref. Data Suppl. **17** (1988), entire volume.
[33] T. P. Fehlner and R. B. Callen, Adv. Chem. Ser. **72**, 181 (1968).
[34] F. Y. Yu, T. M. H. Cheng, V. Kempter, and F. W. Lampe, J. Phys. Chem. **76**, 3321 (1972).
[35] M. T. Bowers, in *Gas Phase Ion Chemistry* (Academic, New York, 1979), Vol. 1.
[36] The nine active orbitals chosen are, in the $HP{-}PH_3^+$ adduct: the σ and σ^* orbitals pertinent to the P–H bond and the singly occupied *p* perpendicular to the P–P bond (P atom carrying one hydrogen); the σ, π, and π' of the PH_3 group, carrying six electrons in the aufbau configuration, as well as their antibonding counterparts, σ^*, π^*, and π'^*. In this space a full CI is performed (8820 configurations) and the molecular orbitals are allowed to

relax. When some nuclear rearrangement occurs, these starting orbitals mix consistently to provide other combinations. For instance, in the rearranged $(H_2P–PH_2)^+$ species, the singly occupied orbital becomes an out-of-phase combination of antiperiplanar P hybrids, while the other active MOs are σ and σ^* couples pertaining to the equivalent P–H bonds. The lone pair associated to the in-phase combination of the same antiperiplanar P hybrids is excluded, and corresponds to a lone pair on the left P in $HP–PH_3^+$.

[37] H. B. Schlegel, J. Chem. Phys. **84**, 4530 (1986).

[38] J. B. Foresman and Æ. Frish in *Exploring Chemistry with Electronic Structure Methods* (Gaussian, Pittsburgh, 1996), p. 64.

[39] J. A. Pople, B. T. Luke, M. J. Frish, and J. S. Binkley, J. Phys. Chem. **89**, 2198 (1985).

[40] L. A. Curtiss, K. Raghavachari, G. W. Trucks, and J. A. Pople, J. Chem. Phys. **94**, 7221 (1991).

[41] J. W. Ochterski, G. A. Petersson, and J. A. Montgomery, Jr., J. Chem. Phys. **104**, 2598 (1996), and references therein.

[42] J. W. Ochterski, G. A. Petersson, and K. B. Wiberg, J. Am. Chem. Soc. **117**, 11299 (1995).

[43] D. H. Williams, in *Mass Spectrometry. A Specialist Periodical Report* (The Chemical Society, London, 1971), Vol. 1.